Biocontrol Science and Technology

ISSN: (Print) (Online) Journal homepage: https://www.tandfonline.com/loi/cbst20

Molecular and biochemical characterisation of antagonistic mechanisms of the biocontrol agent *Bacillus cereus B*25 inhibiting the growth of the phytopathogen *Fusarium verticillioides* P03 during their direct interaction *in vitro*

Paúl Alán Báez-Astorga, Jesús Eduardo Cázares-Álvarez, Abraham Cruz-Mendívil, Francisco Roberto Quiroz-Figueroa, Valeria Isabel Sánchez-Valle & Ignacio Eduardo Maldonado-Mendoza

To cite this article: Paúl Alán Báez-Astorga, Jesús Eduardo Cázares-Álvarez, Abraham Cruz-Mendívil, Francisco Roberto Quiroz-Figueroa, Valeria Isabel Sánchez-Valle & Ignacio Eduardo Maldonado-Mendoza (2022) Molecular and biochemical characterisation of antagonistic mechanisms of the biocontrol agent *Bacillus cereus B*25 inhibiting the growth of the phytopathogen *Fusarium verticillioides* P03 during their direct interaction *in vitro*, Biocontrol Science and Technology, 32:9, 1074-1094, DOI: 10.1080/09583157.2022.2085662

To link to this article: https://doi.org/10.1080/09583157.2022.2085662

BIOCONTROL SCIENCE AND TECHNOLOGY
2022, VOL. 32, NO. 9, 1074–1094
https://doi.org/10.1080/09583157.2022.2085662

Taylor & Francis
Taylor & Francis Group

RESEARCH ARTICLE

Molecular and biochemical characterisation of antagonistic mechanisms of the biocontrol agent *Bacillus cereus B25* inhibiting the growth of the phytopathogen *Fusarium verticillioides* P03 during their direct interaction *in vitro*

Paúl Alán Báez-Astorga [a], Jesús Eduardo Cázares-Álvarez [a], Abraham Cruz-Mendívil [b], Francisco Roberto Quiroz-Figueroa [a], Valeria Isabel Sánchez-Valle[a] and Ignacio Eduardo Maldonado-Mendoza [a]

[a]Departamento de Biotecnología Agrícola, Centro Interdisciplinario de Investigación para el Desarrollo Integral Regional (CIIDIR), Unidad Sinaloa, Instituto Politécnico Nacional, Guasave, Sinaloa, México; [b]CONACYT - Instituto Politécnico Nacional, CIIDIR Unidad Sinaloa, Guasave, Sinaloa, México

ABSTRACT

Fusarium verticillioides (*Fv*) is a mycotoxin-producing phytopathogen causing ear and root rot in maize. *Bacillus cereus* strain *B*25 is a maize endophyte and an effective biological control agent against *Fv*. The *B*25 genome contains several genes associated with fungal antagonism, including lytic enzymes (chitinases A and B, chitosanase and glycoside hydrolase), siderophores (petrobactin and bacillibactin), antibiotics (surfactin), and biofilm. This study aimed to elucidate which *B*25 antagonistic mechanisms are implicated in *Fv* biocontrol. The expression of twelve *B*25 genes was evaluated by qRT-PCR after 3–30 h of confrontation between *B*25 and *Fv*. All *B*25 genes tested were induced, mainly between 6 and 24 h, while none was induced at 3 h. Lytic enzyme genes were induced at different times, with three of them occurring at 12 h. Chitinase and chitosanase activities were induced after 6 and 12 h, respectively, and gradually increased until 30 h. Biofilm formation was detected only when *B*25 interacted with *Fv*. Images of the *B*25-*Fv* interaction and measurements at 24 and 30 h showed little branching or abnormal mycelial growth, suggesting cell wall damage. In conclusion, when *B*25 is confronted against *Fv*, all *B*25 antagonistic mechanisms tested appear to be involved in *Fv* growth control.

ARTICLE HISTORY
Received 10 February 2022
Returned 19 May 2022
Accepted 31 May 2022

KEYWORDS
Biocontrol; qRT-PCR; *Bacillus cereus*; cell wall-degrading enzymes; *Fusarium verticillioides*; bacterium-fungus interaction

1. Introduction

The fungal genus *Fusarium* encompasses a group of plant pathogen species that have an important economic impact on crop production around the world. *Fusarium* represents a human as well as animal health threat, due to its ability to produce mycotoxins, such as

CONTACT Ignacio Eduardo Maldonado-Mendoza ignacioemaldonado@yahoo.com.mx Departamento de Biotecnología Agrícola, Centro Interdisciplinario de Investigación para el Desarrollo Integral Regional (CIIDIR), Unidad Sinaloa, Instituto Politécnico Nacional, Boulevard Juan de Dios Bátiz Paredes # 250, Col. San Joachin, 81101, Guasave, Sinaloa, México

This article has been corrected with minor changes. These changes do not impact the academic content of the article.

the fumonisins produced by *Fusarium verticillioides* (*Fv*) (Deepa et al., 2016). *Fv* is the main pathogen causing ear and root rot in maize around the world (Covarelli et al., 2012; Leyva-Madrigal et al., 2017; Madania et al., 2013). A proposed maize infection mechanism by *Fv* involves the modification of maize chitinases A and B via an effector protein, specifically a secreted protease known as fungalysin or *Fv*-cmp (chitinase-modifying protein). Cmps truncate plant class IV chitinases by cleaving their N-termini (Naumann et al., 2011). The hemibiotrophic lifestyle of this pathogen which acts as both a necrotroph and an endophyte, hinders control strategies using fungicides. In addition, current global concerns demand the use of environmentally safe alternatives. Hence, the use of biological control agents (BCAs) and plant breeding for *Fv* resistance as well as for fumonisin content reduction appear to be the most economic and environmentally safe strategies (Bacon et al., 2001; Maschietto et al., 2016; Shu et al., 2017).

Biological control of plant pathogens is an important tool for integrated pest management (IPM) (Raymaekers et al., 2020). Biocontrol agents include organisms widely found in nature such as bacteria, fungi, viruses, yeast and protozoans (Köhl et al., 2019). As BCAs, bacteria have become an effective and ecofriendly tool in agriculture that can mitigate and/or control the negative effects caused by phytopathogenic fungi in crops (Bacon et al., 2001; Jiang et al., 2016; Lizárraga-Sánchez et al., 2015).

BCAs act against pathogens via several modes of action: by inducing systemic resistance (ISR) or priming in the plant host; by competing for nutrients or modulating the growth conditions for the pathogen; and through parasitism and antibiosis (Köhl et al., 2019). *Bacillus subtilis*, *B. thuringiensis* and *B. cereus* have been used as BCAs to effectively control important plant diseases, including root and ear rot of maize caused by *Fv* (Bacon et al., 2001; Cavaglieri et al., 2005; Jiang et al., 2016; Lizárraga-Sánchez et al., 2015; Reyes-ramírez et al., 2006).

Bacillus cereus sensu lato strain *B*25 is a non-hemolytic (Figueroa-López et al., 2016) maize endophyte bacteria with proven potential to control *Fv in vitro*, as well as in the greenhouse and the field, and the ability to reduce the accumulation of fumonisins and increase grain yield in field trials (Figueroa-López et al., 2016; Lizárraga-Sánchez et al., 2015; Martínez-Álvarez et al., 2016). Massive sequencing of bacterial genomes, particularly those from BCAs, has helped increase our understanding of the genes related to antagonistic mechanisms that could be involved in the biocontrol of plant fungal diseases (Douriet-Gámez et al., 2018). Gene expression and biochemical analysis of these genes could provide a better understanding of how these bacteria exert their biocontrol, and could help find and exploit novel sustainable alternatives for controlling plant pathogens. Several genes in the *B*25 genome are related to the production of a wide variety of antagonistic mechanisms including chitinases, a chitosanase, glycoside hydrolases, siderophores, antibiotics, and biofilm (Douriet-Gámez et al., 2018). Some of these mechanisms were previously identified by biochemical tests (Figueroa-López et al., 2016). Gene expression of *B*25 chitinase genes (*ChiA* and *ChiB*) was evaluated by qRT-PCR in an experiment using colloidal chitin and fungal lysate as bacterial chitinase gene inducers (Figueroa-López et al., 2017). In addition, the *B*25 ChiA and ChiB proteins were heterologously expressed in *E. coli*, purified and biochemically characterised (Morales-Ruiz et al., 2021). ChiA possesses exochitinase activity, while ChiB has both exochitinase and endochitinase activity. Whether alone or in combination, the two purified recombinant enzymes have been shown to reduce *Fv* conidia germination *in vitro*, by affecting their growth patterns. This produces swollen and

unbranched mycelia, suggesting that *B*25 chitinases play a key role in *Fv* germination and growth control (Morales-Ruiz et al., 2021).

Despite the currently available information on *B. cereus B*25, the molecular interactions between *B*25 and *Fv* are still not well understood, and it remains unclear which antagonistic mechanisms of *B*25 are implicated in the biological control responses when challenged with *Fv*. Therefore, in this work we aimed to study the *B*25-*Fv* interaction from a molecular and biochemical point of view, in order to improve our understanding of the antagonistic mechanisms implicated in the biological control exerted by *B*25 over *Fv*.

2. Materials and methods

2.1. Microorganisms and inoculum preparation

Bacillus cereus sensu lato strain *B*25 and *Fusarium verticillioides* strain P03 were used in this study. *B*25 was previously isolated from the maize rhizosphere of commercial maize fields in Guasave, Sinaloa, Mexico, and initially identified on the basis of its 16S rDNA sequence (Figueroa-López et al., 2014, 2016). Later, when its genome was sequenced, phylogenomic analysis confirmed it as a member of the *B. cereus* group, and it was finally named *B. cereus sensu lato* (Douriet-Gámez et al., 2018). *B*25 was reactivated from a frozen stock (−70°C) by growing it on Luria Bertani (LB) agar at 30°C for 24 h. A single colony was picked and grown in a tube containing 5 mL of LB broth at 30°C with orbital shaking at 200 rpm for 24 h. Next, 1 mL of this culture was transferred to a 250-mL Erlenmeyer flask containing 100 mL of half-strength LB broth and incubated under the previous conditions. This final culture was used as an inoculum for the confrontation assay.

Fv P03 was previously isolated from maize roots with rot symptoms in a field in El Fuerte Valley, Sinaloa, Mexico, and subsequently its identity was established both morphologically and molecularly (Leyva-Madrigal et al., 2015). The pathogenicity of this isolate was previously tested and confirmed in different studies (Figueroa-López et al., 2014, 2016; Leyva-Madrigal et al., 2015, 2017; Lizárraga-Sánchez et al., 2015; Martínez-Álvarez et al., 2016). *Fv* P03 was reactivated from a frozen stock (−70°C) by growing it on PDA plates at 25°C for 10 days. Conidia were harvested using sterile distilled water. Subsequently, a 250-mL Erlenmeyer flask containing 100 mL of half-strength LB was inoculated with conidia for a final concentration of 10^6 conidia mL^{-1} and incubated at 30°C with orbital shaking at 200 rpm for 24 h. Mycelia obtained from this culture were used as an inoculum for the confrontation assay. The mycelia weight inoculated in the flasks was calculated using three aliquots of 1 mL of mycelia. Supernatant was discarded after centrifugation (9,200 g for 1 min) and the remaining mycelia were dried at 50°C for 30 h, and finally weighed using an analytical balance (HR-150AZ, A&D Company, Limited, Tokyo, Japan). The mean weight was used to extrapolate the volume of the mycelia suspension used as an inoculum.

2.2. Confrontation assay

A confrontation assay between *B*25 and *Fv* was performed in order to evaluate the transcript levels of the bacterial genes involved in antagonistic mechanisms when the bacteria

comes into direct contact with the phytopathogen. Three conditions were established: two controls (*B*25 and *Fv*) and one treatment (*B*25 + *Fv*). Treatment consisted of several 250-mL Erlenmeyer flasks containing 100 mL of half-strength LB broth inoculated with both *B*25 and *Fv* prepared as described in the previous section. Initial inoculum concentrations were 2×10^6 colony forming units (CFU) mL^{-1} for *B*25 and 0.015 mg mL^{-1} of mycelia for *Fv*. Controls consisted of flasks containing the culture media inoculated with either *B*25 or *Fv*. Briefly, the growing conditions were 30°C with orbital shaking at 200 rpm. This experiment was conducted using three biological replicates.

Aliquots (1.5 mL) were taken from each condition at 3, 6, 12, 24 and 30 h and transferred to 2-mL tubes. Next, the samples were centrifuged at 1,800 g and 4°C for 5 min, and then cell pellets were separated from supernatant by decanting the supernatant in new 2-mL tubes. Cell pellets and supernatants were immediately frozen in liquid nitrogen, and cell pellets were subsequently ground in a mixer mill (Tissue Lyser II, Qiagen, Cat. No. 85300, Hilden, Germany). Next, both preparations were stored at −70°C until used.

At each of the previously stated sampling times, 0.1-mL aliquots of the microorganism suspensions were taken in order to monitor the bacterium-fungus interaction during the interaction assay under the light microscope.

2.3. qRT-PCR analysis

Cell pellets from the confrontation assay were used for RNA extraction. Total RNA was isolated using TRIzol Reagent (Thermo Fisher Scientific, Cat. No. 15596-026, Waltham, MA) according to the manufacturer's instructions. The amount and quality (260/280 nm ratio) of the total RNA were estimated by spectrophotometry using a Nanodrop 2000c (Thermo Fisher Scientific, Wilmington, DE, USA), and integrity was determined by agarose gel electrophoresis (Aranda et al., 2012). Total RNA was treated with RQ1 DNase (PROMEGA, Cat. No. M6101, Fitchburg, WI, USA) to avoid DNA contamination. An end point PCR was performed after DNase treatment to confirm the absence of DNA contamination. First-strand cDNA was synthesised from 1 µg of total RNA using SuperScript III reverse transcriptase (Thermo Fisher Scientific, Cat. No.18080-044, Waltham, MA, USA), following the manufacturer's instructions. Reagents and qRT-PCR conditions were prepared as in Cervantes-Gámez et al. (2015) with slight modifications. qRT-PCR reactions were performed in duplicate for each of the three biological replicates in a Rotor Gene-Q Real time PCR system (Qiagen, Cat. No. 9001550, Hilden, Germany). Reactions included 5 µL of SYBR Green master mix (Qiagen, Cat. no. 204074, Hilden, Germany), 1 µM of each primer, 10 ng of cDNA, and RNase-free water for a final volume of 10 µL. For PCR amplification, the thermocycler programme included a preheating step at 95°C for 5 min, followed by 40 cycles of denaturation at 95°C for 30, 30 s annealing at 54°C, and 20 s extension at 72°C. Dissociation curves were performed at the end of each run to confirm single-product amplifications. Gene-specific primers were downloaded from the literature or designed in the Primer3 programme, using the available *B*25 genome (Douriet-Gámez et al., 2018) (Table 1). PCR amplification efficiency of the housekeeping and target genes was determined from standard curves constructed from serial dilutions of cDNA (from 1 to 100 ng). Relative quantification of bacterial genes was normalised to the

housekeeping gene *rpsU* (30S ribosomal protein 21), and fold change (FC) values in gene expression were calculated using the comparative threshold cycle method $2^{-\Delta\Delta Ct}$ (Livak & Schmittgen, 2001).

2.4. Lytic enzyme activity: chitinases and chitosanase

The enzymatic activity of chitinases and chitosanase was evaluated in the supernatants from the confrontation assay. Before their use, supernatants were filtered through a 0.22 μM filter to avoid bacterial and fungal contamination.

2.4.1. Chitinase activity

Chitinase activity was determined using a fluorometric chitinase assay kit (Sigma Aldrich, Cat. No. CS1030, St. Louis, MO, USA) based on the enzymatic hydrolysis of the chitin substrates bound to 4-methylumbelliferone (4-MU). One unit of chitinase activity was defined as the amount of enzyme required to release 1 μmol of 4-MU from the substrate per minute at pH 5.0 and 37°C. The specific endochitinase and exochitinase activities were assayed using three different substrates provided with the chitinase assay kit described above: the monomer N-acetyl-β-D-glucosaminide (GlcNAc) and the dimer N,N'-diacetyl-β-D-chitobioside (GlcNAc-2) for exochitinase activity, and the trimer β-D-N,N',N''-triacetylchitotriose (GlcNAc-3) for endochitinase activity. Enzymatic assays were performed according to the manufacturer's instructions. Each type of enzymatic activity was assayed using three biological replicates (supernatant aliquots from three different flasks) with two technical replicates each (n = 6).

2.4.2. Chitosanase activity

Chitosanase activity was evaluated using the chitosanase-detection agar (CDA) plate with modifications (Cheng & Li, 2000). One litre of CDA medium was prepared by mixing 4 g

Table 1. List of qRT-PCR primers for *B. cereus B*25 genes related to antagonistic mechanisms against phytopathogenic fungi. All primers had a melting temperature of 54°C.

Category	Gene	Forward (5′→3′)	Reverse (5′→3′)	Reference
Siderophores	*BcdhbA*	GGGGCAATTGTTACAGTCGG	GTATGCCGCAAGCTCTAGTC	This study
	BcAsbA	GCAACATCATCACTAAGGACG	GCAACATCATCACTAAGGACG	This study
	BcAsbB	GTATTGAAGGCGCTCGAATC	CCGGTGTAATAATCCCCTC	This study
Lytic enzymes	*BcChiA*	CCTTTCCAAGCACAAGCAG	TCCCATTTTGGTGAAACGTC	Figueroa-López et al. (2017)
	BcChiB	TCAGGGACAACTTGGGAAG	CCAAGTCCAGCCACCAAC	Figueroa-López et al. (2017)
	BcCsn	CACAACCCGCACCTAAAGAC	CGCCGTACATCGCATAGTCC	This study
	BcGH18	GACATACGACTGGGGATGGC	TTGCGGGTGGATTTCCTTGT	This study
Biofilm formation	*BcTasA*-like1	GGTGAAGACTTTGGTAAGCACG	CTCCCCACTCAGGAGCGAAG	This study
	BcTasA-like2	GTTGGTGGAGGAACATTTGC	CGATACGTTAACAACCGTTGATG	This study
Antibiotics	*BcSrfAA*	GATACTTGGACGCTTTTTCA	TAATCCAGTACGGAACAACA	This study
	BcSrfAD	TAGATGATTCGCCCTACATT	GATTTCTACCGGACAAAACA	This study
	Bcsfp	CCGATCTCTAATCTGCCAAA	GTAGTACAAACCACCCATTC	This study
Normalizer gene	*rpsU*	GTCTTTGGAGGATGCACTTCG	GCTTTCTTGCCGCTTCAGAT	Reiter et al. (2011)

of chitosan (Sigma-Aldrich, USA, Cat. No, C3646) pre-dissolved in 200 mL of 1% acetic acid, 20 g agar and M9 medium salts: Na_2HPO_4 (1.3 g), KH_2PO_4 (3.0 g), NaCl (0.5 g), NH_4Cl (1.0 g), $MgSO_4$ (0.24 g) and $CaCl_2$ (0.01 g). The final pH was adjusted to 6.5 with NaOH. Ten 3-mm diameter wells were made (three wells for each control (*B*25 and *Fv*) and treatment (*B*25 + *Fv*), and one well for a negative control) per CDA plate with a cork borer. Next, wells were filled with 25 µL of supernatant from each condition (controls and treatment) and the negative control well was added with 25 µL of half-strength LB broth. CDA plates were incubated at 25°C for 24 h and chitosanase activity was detected and recorded by the presence of a clear zone (measured in mm) formed around the wells filled with the supernatants. A single CDA plate was used to evaluate the chitosanase activity of all conditions (controls and treatment) for each sampled time point. Five CDA plates were used to evaluate the chitosanase activity of all conditions and sampled time points (3, 6, 12, 24 and 30 h). This experiment was performed twice, each time with the supernatant from three biological replicates for each condition (n = 6).

2.5. Biofilm formation assay

To assess biofilm formation in *B*25 when interacting with *Fv*, the microtiter plate biofilm assay was performed with some modifications (Auger et al., 2006). *B*25 and *Fv* inocula for this assay were prepared as in section 2.1. Two pre-inoculum dilutions for each microorganism were prepared in LB broth medium: a 1:100 (v/v) dilution for controls (*B*25 and *Fv* growing alone) and a 1:50 (v/v) dilution for the *B*25 + *Fv* treatment, in order to obtain equal amounts of the microorganisms in all conditions. For controls, 200 µL of each diluted culture (1:100) was added to six wells of a 96-well plate, whereas for the *B*25 + *Fv* treatment a mixture of 100 µL of each culture (1:50) was added. Culture media with no microorganisms was included as a negative control in this experiment. Plates were incubated statically at 30°C for 3, 6, 12, 24, 30 and 48 h. A single plate was used to evaluate all sampled time points. The supernatant was discarded and the adhered cells were rinsed once with phosphate-buffered saline (PBS) solution. Plates were dried at room temperature for 1 h. Next, 200 µL of 1% crystal violet (CV) solution was added to each well and incubated for 20 min at room temperature. The CV solution was discarded and each well was rinsed three times with PBS. Plates were dried at room temperature for 1 h. Next, 200 µL of 96% ethanol was added to each well and incubated for 15 min to release the bound CV dye from the biofilm. Finally, 125 µL of this solution was transferred to a new 96-well plate for quantification at an absorbance of 595 nm (A_{595}).

2.6. Conidia germination inhibition assay

To evaluate the effect that the bioactive compounds secreted by the bacterium – in response to its interaction with *Fv* – have over the germination of *Fv* conidia, supernatants from the confrontation assay with the *B*25 + *Fv* treatment were used and compared to those from the controls (*B*25 and *Fv*). This experiment was performed in 1.5-mL sterile tubes in a final volume of 100 µL, containing one part potato dextrose broth (PDB) 2X and one part supernatant (v/v), with a total of 1×10^3 conidia. As a

negative control, we used half-strength LB broth instead of supernatant. Tubes were incubated at 30°C for 48 h. After the incubation, conidia germination was determined based on the visualisation of 100 conidia observed under a light microscope (Axiostar 1061-030, Carl Zeiss) with a Neubauer chamber. The percentage of germination was assessed with the following formula:

$$\%\text{of germination} = \frac{\text{germinated conidia}}{\text{observed conidia}} \times 100$$

The experiment was performed twice with three biological replicates (independent tubes) for each sampling point, and the mean of the percentage of germination was reported (n = 6).

2.7. Time course of the bacterium-fungus direct physical interaction

2.7.1. Analysis of the direct interaction between B25 and Fv by light microscopy

10-µL of sample from the 0.1-mL aliquots taken from each condition and time during the interaction assay (section 2.2.) were placed on slides and carefully dried under a flame. Next, the dried samples were covered with 0.5% safranin for 30 s for staining and then washed with distilled water to remove the excess of safranin. Stained samples were observed under a light microscope at 40X and imaged. The number of branches per 80 µm of *Fv* hyphal segment were counted in the *B*25 + *Fv* treatment and the *Fv* control.

2.7.2. Analysis of the direct interaction between B25 and Fv by confocal laser microscopy

In order to visualise the effect of *B*25 on the mycelium structure and growth of the fungal phytopathogen, an independent experiment was performed using a *B*25 transformant strain carrying the plasmid pAD4325. This harbours a gene coding for GFP, which allows visualising the bacterium, while also conferring resistance to ampicillin and chloramphenicol (Morales-Ruiz et al., 2019). The conditions for this experiment were the same as in the confrontation assay (section 2.2.), with the exception that 5 µg mL^{-1} chloramphenicol was added to the media in order to avoid plasmid loss. Controls without antibiotics were included in this experiment. Samples (10 µL aliquots) were taken at 3, 6, 12, 24 and 30 h. Immediately after samples were taken, they were placed on a 1-cm^2 agarose pad (UltraPure™ Low Melting Point Agarose, Thermo Fisher Scientific, Waltham, MA, USA), covered with a coverslip, and imaged. The samples were visualised in a Leica TCS SP5 X confocal laser microscope using a white laser with 499 nm as the excitation wavelength, and emission was detected in a range of 512–526 nm.

2.8. Statistical analysis

Statistical analysis was performed using the IBM SPSS Statistics 25 programme. Chitinase activity, biofilm formation and the conidia germination inhibition assay were analyzed by one-way ANOVA. Differences among treatments were determined by Tukey's test at a significance level of $P = 0.05$. Chitosanase activity and mycelia branching number were analyzed by Student's t test at a significance level of $P = 0.05$.

3. Results

3.1. qRT-PCR analysis

The gene expression analysis of the genes related to antagonistic mechanisms in *B*25 against *Fv* showed that all genes were upregulated (FC > 2) at most of the evaluated sampling times (Figure 1). Almost all of the genes were induced between 6 and 24 h, and no gene was induced at 3 h. Seven of the genes (*BcAsbA*, *BcAsbB*, *BcChiA*, *BcChiB*, *BcCsn*, *BcGH18* and *BcSrfAA*) were repressed in at least one of the evaluated time points, typically at 3 h.

3.1.1. Siderophore synthesis genes

BcdhbA is a member of the *dhbABCEF* operon and is involved in bacillibactin synthesis. *BcdhbA* was induced from 6 to 24 h, and had the highest FC value (3.45) at 12 h (Figure 1A).

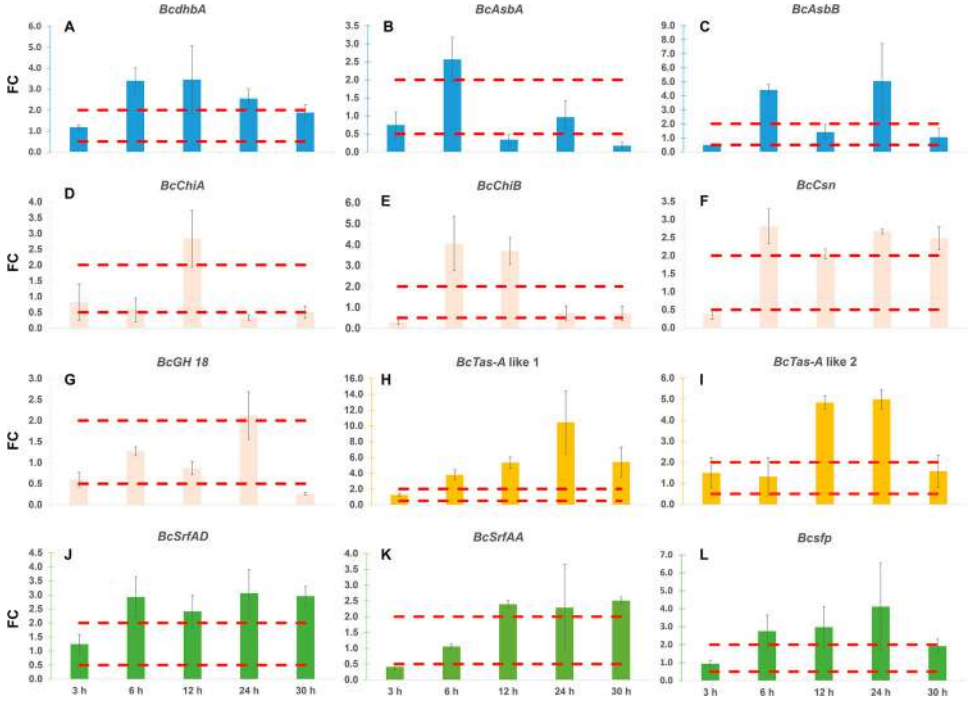

Figure 1. Expression analysis by qRT-PCR of *Bacillus cereus B*25 genes related to diverse antagonistic mechanisms, during a time course experiment of a direct liquid confrontation assay against *Fv*. Data were normalised to *rpsU* and reported as fold change (FC) values relative to a *B*25 control growing alone (*B*25-*Fv*/*B*25). The different colours in the bar charts represent genes from different categories/antagonistic mechanisms. Blue indicates siderophore-related genes: A) *BcdhbA*, B) *BcAsbA* and C) *BcAsbB*. Pink shows the expression patterns of genes encoding enzymes involved in fungal cell wall degradation: D) *BcChiA*, E) *BcChiB,* F) *BcCsn*, and G) *BcGH18*. Yellow refers to genes involved in biofilm formation: H) *BcTasA*-like 1 and I) *BcTasA*-like 2. Finally, green indicates surfactin-related genes: J) *BcSrfAD*, K) *BcSrfAA* and L) *Bcsfp*. The vertical lines in each bar indicate the standard deviation of the FC values, and the horizontal dotted red lines in each plot refer to FC values of 2 (upper line) or 0.5 (lower line). The values indicate the average of three biological replicates with two technical replicates (n = 6).

BcAsbA and *BcAsbB* are members of the *asbABCDEF* operon and are involved in petrobactin synthesis. Both genes were induced at 6 h, however, only *BcAsbB* was induced again at 24 h (Figure 1B-C).

3.1.2. Cell wall degradation genes

BcChiB (Figure 1E) and *BcCsn* (Figure 1F) were both repressed at 3 h with FC values of 0.29 and 0.38, respectively. Subsequently, they were both induced at 6 h with FC values of 4.04 and 2.81, respectively. *BcChiA* (Figure 1D) and *BcChiB* (Figure 1E) were both induced at 12 h, whereas *BcGH18* (Figure 1G) was induced until 24 h (FC = 2.12) and then repressed at 30 h (FC = 0.26).

3.1.3. Biofilm formation genes

BcTasA-like 1 and *BcTasA*-like 2 are both part of the *sipW-tasA* operon and are involved in biofilm formation. *BcTasA*-like 1 (Figure 1H) was induced from 6 to 30 h, and *BcTasA*-like 2 (Figure 1I) was induced at 12 and 24 h. Remarkably, *BcTasA*-like 1 presented the highest FC value (10.45) out of all genes evaluated, at 24 h.

3.1.4. Antibiotic production genes

BcSrfAD, BcSrfAA and *Bcsfp* are genes from the *srf* operon for surfactin biosynthesis, and all presented a similar pattern of induction. *BcSrfAD* (Figure 1J) was induced from 6 to 30 h, *BcSrfAA* (Figure 1K) was induced from 12 to 30 h, and *Bcsfp* (Figure 1L) was induced from 6 to 24 h. Only *BcSrfAA* was repressed at 3 h (FC = 0.41; Figure 1K).

3.2. B25-Fv physical interaction

Light and confocal laser microscopy images of samples from the confrontation assays showed the growth inhibitory effect of *B*25 on *Fv* mycelia starting at 3 h and lasting until 30 h in the *B*25 + *Fv* treatment (Figures 2 and 3). A lower (but not significant) fungal hyphae branch count was observed at 6 h in the *B25 + Fv* treatment (4.33 branches per 80-µm hyphal segment) as compared to the *Fv* control (6.90 branches per 80-µm hyphal segment) (Figure 2; Table 2). At both 24 and 30 h, a very low branch count (0.53 and 0.6 branches per 80-µm hyphal segment) was observed in the *B25 + Fv* treatment, whereas the *Fv* control displayed a significantly higher branch count (6.70 and 5.10 branches per 80-µm hyphal segment) (Table 2). Moreover, abnormal *Fv* mycelium growth, including thinning of the cell wall and swelling of the hyphae, was observed at 24 and 30 h (Figures 2 and 3).

Table 2. Branching of *Fv* mycelia during the confrontation assay between *Fv* and *B. cereus B*25.

	Number of branches per *Fv* hyphal segment	
Time	*Fv*	*B25 + Fv*
6 h	6.90 ± 0.95	4.33 ± 0.31
12 h	6.20 ± 0.72	4.00 ± 0.87
24 h	6.67 ± 1.10	0.53 ± 0.12*
30 h	5.13 ± 0.42	0.60 ± 0.00*

* indicates significant differences compared to the *Fv* control at a given time (Student's t-test, $P < 0.05$). Values indicate the mean number of branches in 15 hyphal 80-µm segments from three biological replicates (five hyphal segments per biological replicate). Data are presented as mean ± standard deviation.

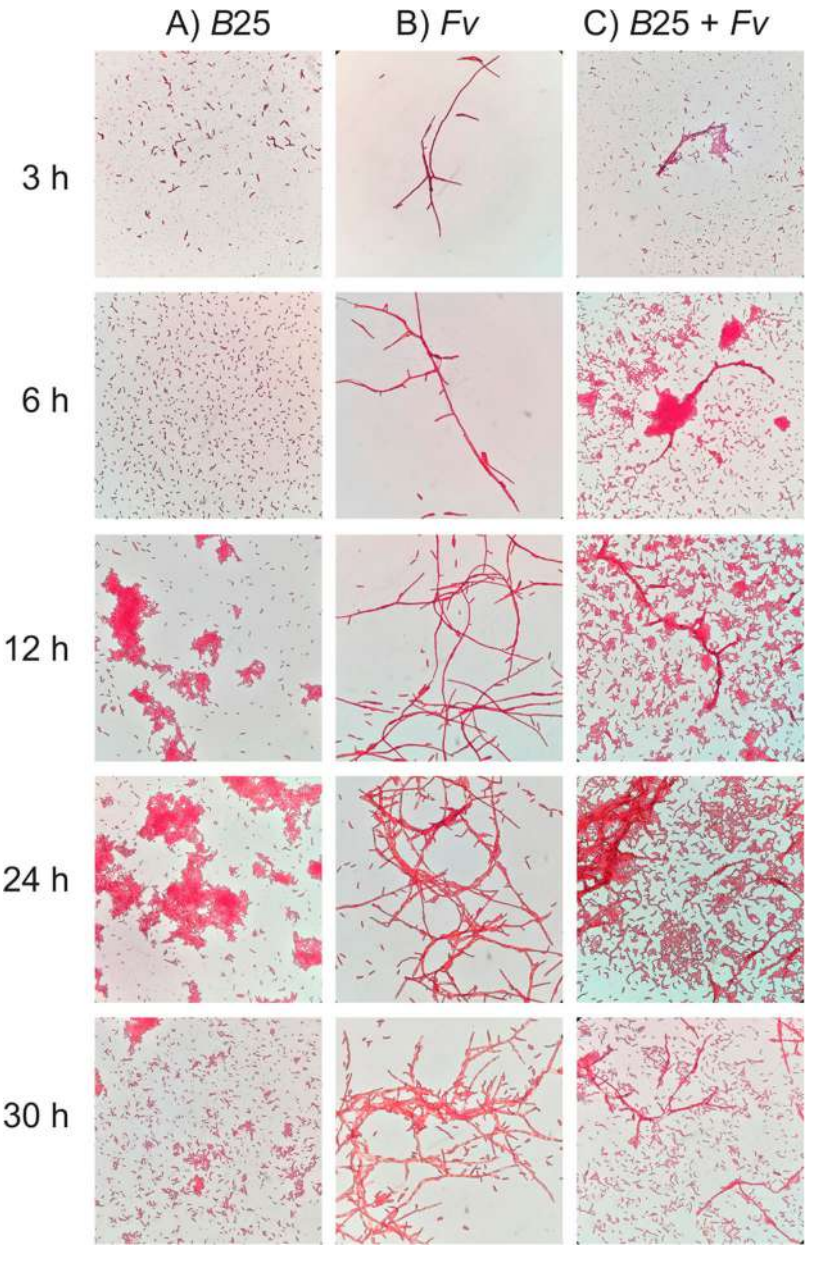

Figure 2. Microscopic visualisation of samples from the direct confrontation assay between *B*25 and *Fv* in liquid culture. All samples (*B*25, *Fv*, and *B*25 + *Fv*) were observed at 3, 6, 12, 24 and 30 h. Micrographs were taken under a light microscope at 40X.

3.3. Chitinase activity

Exochitinase activity of the supernatants evaluated in the GlcNAc monomeric substrate showed less than 10 U/mL of chitinase activity for all samples, except for the *Fv* control at 24 and 30 h, which presented values of 34.8 and 29.1 U/mL of chitinase activity,

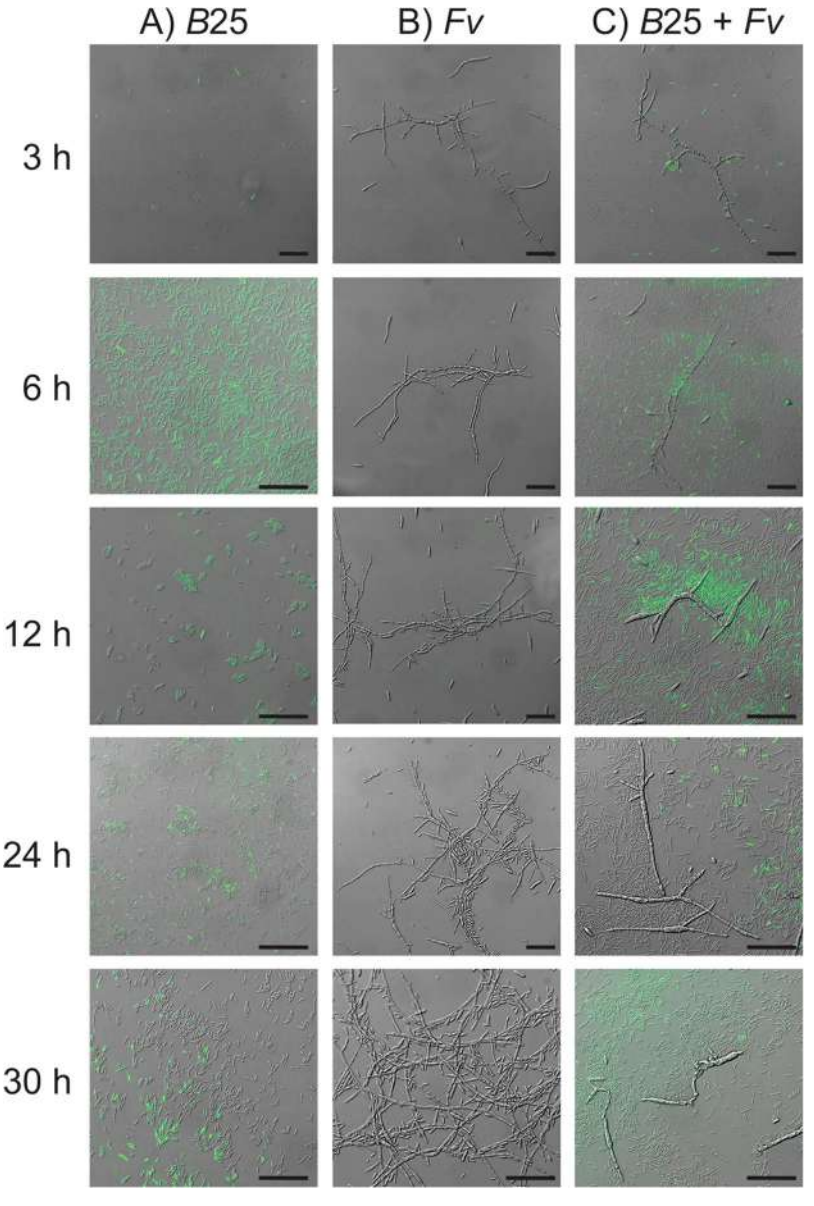

Figure 3. Microscopic visualisation of samples from the direct confrontation assay between *B25* carrying the plasmid pAD4325 (coding for GFP) and *Fv* in liquid culture. All samples (*B25*, *Fv*, and *B25* + *Fv*) were observed at 3, 6, 12, 24 and 30 h. Micrographs were taken under a confocal laser microscope at 40X. The scale bar at the bottom right of each panel indicates 50 µm.

respectively (Table 3). Interestingly, in this substrate (GlcNAc), the chitinase activity in the interaction samples (treatment *B25* + *Fv*) was significantly lower than in the *Fv* control samples, except at 3 h. These differences were more evident at 24 and 30 h, since the values from the *B25* + *Fv* treatment were approximately four times smaller (8.2 and 7.3U/mL) than in the *Fv* control samples.

Table 3. Chitinase activity in the supernatants of samples from the confrontation assay between *B. cereus B*25 and *Fv*.

	Chitinase activity (U/ml)								
	Exochitinase						Endochitinase		
	GlcNAc			GlcNAc-2			GlcNAc-3		
Time	*B25*	*Fv*	*B25 + Fv*	*B25*	*Fv*	*B25 + Fv*	*B25*	*Fv*	*B25 + Fv*
3 h	2.4 ± 0.1^{b}	4.4 ± 0.3^{a}	3.9 ± 0.3^{a}	0.2 ± 0.1^{a}	0.5 ± 0.3^{a}	5.8 ± 4.4^{a}	1.2 ± 0.2^{b}	1.4 ± 0.1^{b}	2.1 ± 0.4^{a}
6 h	2.3 ± 0.2^{c}	5.0 ± 0.4^{a}	4.3 ± 0.1^{b}	0.7 ± 0.6^{b}	0.5 ± 0^{b}	240.6 ± 23^{a}	1.5 ± 0.4^{b}	2.3 ± 0.2^{b}	33.2 ± 3.7^{a}
12 h	1.4 ± 0.3^{b}	4.6 ± 1.2^{a}	2.0 ± 0.1^{b}	1 ± 0.5^{b}	1.6 ± 0.3^{b}	702.2 ± 56.2^{a}	1.5 ± 1.0^{b}	11.0 ± 0.8^{b}	132.8 ± 11.3^{a}
24 h	3.1 ± 0.4^{c}	34.8 ± 1.9^{a}	8.2 ± 1.2^{b}	2972.4 ± 22.8^{a}	3.5 ± 0.4^{c}	2621.1 ± 39.1^{b}	1218.3 ± 163.3^{a}	25.6 ± 1.3^{c}	848.5 ± 39.2^{b}
30 h	1.9 ± 0.1^{c}	29.1 ± 0.5^{a}	7.3 ± 3.5^{b}	3046.3 ± 6.6^{a}	3.5 ± 0.3^{c}	2918 ± 9.3^{b}	1115.5 ± 30.8^{a}	25.2 ± 1.3^{c}	1012.2 ± 20.2^{b}

The effects of three different substrates were examined: N-acetyl-β-D-glucosaminide (GlcNAc); N, N′-diacetyl- β-D-chitobioside (GlcNAc-2) for exochitinase activity; and β-D-N, N′, N″-triacetyl-chitotriose (GlcNAc-3) for endochitinase activity. Different superscript letters in the same row indicate significant differences between conditions at a given time and within each chitinase substrate (Tukey's test, $P<0.05$). U: a unit is defined as the amount of enzyme needed to release 1 µmol of 4-methylumbelliferone from the substrate per minute at pH 5.0 and 37°C. Values indicate the mean of three biological replicates in duplicate (n = 6). Data are presented as mean ± standard deviation.

The *B*25 and *Fv* control samples in GlcNac-2 substrate (exochitinase activity) displayed very low chitinase activity values (<2 U/mL) between 3 and 12 h (Table 3). In contrast, the exochitinase activity values of the *B*25 + *Fv* samples were significantly higher than the controls at 6 and 12 h (240.6 and 702.2 U/mL). The exochitinase activity in the *B*25 control and *B*25 + *Fv* treatment samples exceeded 2,600 U/mL at 24 and 30 h, whereas the activity in the *Fv* control sample remained low (< 4 U/mL). Finally, the exochitinase activity of the *B*25 samples in GlcNac-2 substrate was significantly higher at 24 and 30 h than the *B*25 + *Fv* samples.

Endochitinase activity was measured using GlcNac-3 as a substrate. Low endochitinase activity values (≤11 U/mL) were observed for the *B*25 and *Fv* control samples from 3 to 12 h. Consistent with the increase in exochitinase activity in the *B*25 + *Fv* treatment samples at 6 and 12 h in the GlcNac-2 substrate, endochitinase activity in the GlcNac-3 substrate was also significantly higher in this treatment than the *B*25 and *Fv* controls. The highest endochitinase activity values were observed at 24 and 30 h in the *B*25 sample (1218.3 and 1115.5 U/mL) and the *B*25 + *Fv* sample (848.5 and 1012.2 U/mL) (Table 3). Finally, endochitinase activity was significantly higher in *B*25 grown alone as compared to the *B*25 + *Fv* treatment at 24 and 30 h, as similarly observed in GlcNac-2 substrate.

3.4. Chitosanase activity

No chitosanase activity was detected in *Fv* samples at any time, or in *B*25 and *B*25 + *Fv* samples at 3 and 6 h. At 12 and 30 h, the *B*25 + *Fv* sample showed a significantly higher chitosanase activity (9.17 and 14.25 mm) than the *B*25 sample (0 and 13.75 mm) (Table 4).

3.5. Biofilm formation

Results from the microtiter plate assay showed no visual evidence of biofilm formation in *B*25 samples at any of the evaluated times, or in *B*25 + *Fv* samples from 3 to 12 h (Figure 4B). For the *B*25 samples, absorbance values at 595 nm remained stable (0.058 - 0.068) across the evaluated times (Figure 4A), and did not differ from the negative control (data not shown, average = 0.062). On the other hand, absorbance values of the *B*25 + *Fv* samples from 6 to 48 h were significantly higher than those of the *B*25 samples (Figure 4A). However, biofilm formation in the *B*25 + *Fv* samples was only visually evident from 24 to 48 h (Figure 4B).

Table 4. Chitosanase activity in the supernatants of samples from the confrontation assay between *Fv* and *B. cereus B*25.

	Chitosanase activity (halo in mm)	
Time	*B*25	*B*25 + *Fv*
12 h	0	9.17 ± 0.26*
24 h	12.17 ± 1.69	13.33 ± 0.98
30 h	13.75 ± 0.27	14.25 ± 1.04*

* indicates significant differences between conditions at a given time (Student's t-test, $P < 0.05$). Values indicate the mean of three biological replicates from two experiments (n = 6). Data are presented as mean ± standard deviation.

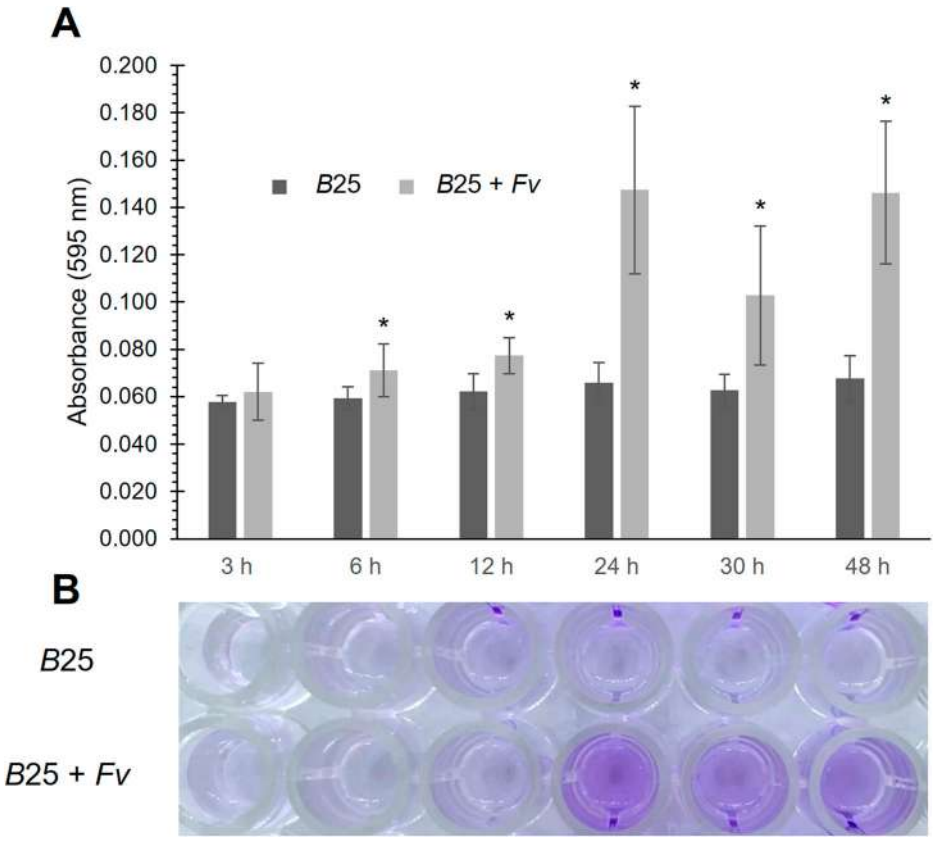

Figure 4. Time course experiment of biofilm staining with crystal violet (CV) for *B25* grown alone or together with *Fv* in microtiter plates. A) Absorbance values at 595 nm for biofilm biomass stained with 1% CV and dissolved in 96% ethanol. B) Representative image of the stained biofilms in the wells of the microtiter plates over time. *indicates significant differences between conditions at a given time (Tukey's test, $P < 0.05$). Bars indicate standard deviation from six samples.

3.6. Inhibition of conidia germination

Supernatants of the *B25 + Fv* treatment from 3, 6, 24 and 30 h showed significant reduction of conidia germination as compared to the *Fv* control and the negative control (conidia incubated in culture media) (Table 5). The highest inhibition percentages were observed for conidia incubated with the supernatant of *B25 + Fv* of 24 and 30 h (29.7 and 29.3% of germinated conidia, respectively). Interestingly, the supernatant of the same fungus (*Fv*) from 3 and 6 h showed a significant reduction in conidia germination as compared to the negative control.

4. Discussion

In previous research, *B. cereus B25* showed the potential to produce siderophores, chitinases, glucanases and proteases for biocontrol against *Fv in vitro* (Figueroa-López et al., 2016). Of these mechanisms, two chitinase genes (*ChiA* and *ChiB*) were found to be

Table 5. Inhibition of conidia germination in *Fv* after 48 h of incubation with supernatants from the confrontation assay between *B25* and *Fv*.

	Percentage of Germination					
		Supernatant				
Treatment		3 h	6 h	12 h	24 h	30 h
B25		34.3 ± 3.2^{bc}	37.7 ± 6^{b}	42.3 ± 2.1^{b}	31.3 ± 1.5^{b}	37 ± 5.6^{bc}
Fv		45 ± 2^{b}	42 ± 5.3^{b}	51 ± 6^{ab}	56.3 ± 6.5^{a}	45.7 ± 4.2^{ab}
B25 + *Fv*		32 ± 4.6^{c}	37.3 ± 4.6^{b}	46.3 ± 2.5^{ab}	29.7 ± 4.2^{b}	29.3 ± 5.8^{c}
Negative control	57.3 ± 6.7^{a}	–	–	–	–	–

Different superscript letters in the same column indicate significant differences between treatments and control at a given time (Tukey's test, $P<0.05$). Values indicate the mean of three biological replicates from two experiments (n = 6). For the negative control, half-strength LB culture medium was added and then harvested like the treatments at 48 h.

inducible by colloidal chitin and fungal lysate (Figueroa-López et al., 2017). Later, sequencing of the *B25* genome confirmed the presence of genes involved in fungal antagonism, including: two siderophores (petrobactin and bacillibactin), two chitinases (ChiA and ChiB), a chitosanase and a glycoside hydrolase involved in fungal cell wall degradation, an antibiotic (surfactin), and genes related to biofilm formation (Douriet-Gámez et al., 2018).

Here, we confirmed that the expression of *B25* genes related to fungal antagonism is induced when *B25* interacts with the maize pathogen *Fv* in liquid culture, mainly between 6 and 24 h into their direct interaction (Figure 1).

Siderophores are iron-chelating agents secreted by bacteria and fungi to acquire iron, an essential element for living organisms (Lee et al., 2011). In addition to their primary role in increasing iron availability, siderophores constitute a mechanism of competition since the siderophore-sequestered iron becomes unavailable to cells without the necessary uptake receptor, consequently causing a growth inhibitory effect (Schiessl et al., 2017). Furthermore, it was previously shown that siderophore-producing *Bacillus* species inhibit the growth of different fungal phytopathogens (Dunlap et al., 2015; Li et al., 2014). In our study, the earliest time at which we found repression (FC = 0.49) for *BcAsbB* (in the *asbABCDEF* petrobactin biosynthetic operon) was at 3 h, and there was no induction for *BcAsbA* (same operon) or *BcdhbA* (in the *dhb* bacillibactin biosynthesis operon) (Figure 1A-C). These three genes were induced at 6 h, but only *BcdhbA* remained induced until 24 h (Figure 1A), suggesting that the production of bacillibactin could be the main mechanism for iron uptake in this bacterium-fungus interaction. However, petrobactin activity could not be ruled out, since the *BcAsbB* transcript expression levels are higher than the other genes, and its expression fluctuates as if it were turned on (6 and 24 h) and turned off (12 and 30 h) (Figure 1C). In *B. anthracis*, *dhbC* (*dhb* operon) and *AsbB* (*asb* operon) transcription is regulated by iron concentration, and low levels of iron induce the expression of both genes (Lee et al., 2011). The overlap in induction for *BcAsbB* and *BcdhbA* at 24 h, in addition to the overlap of the three genes (including *BcAsbA*) at 6 h, suggests that *B25* could use bacillibactin and petrobactin together when *B25* is challenged with *Fv*. Although no induction at 24 h was observed for *BcAsbA* (*asb* operon), it has been demonstrated in *B. anthracis* that even in the absence of *Asb*A induction in the ΔasbA mutant strain, the induction of *AsbB* still allowed production of petrobactin, albeit at a lower level than in the wild

type strain (Lee et al., 2007). Thus, it is possible that petrobactin could be produced at 24 h since *BcAsbB* but not *BcAsbA* was induced at this time. Nevertheless, measurements of both petrobactin and bacillibactin are still needed in order to understand the contribution of siderophores to fungal growth inhibition.

Excretion of cell wall-degrading enzymes (CWDEs) is involved in parasitism, and is a direct biocontrol mechanism employed by some BCAs. This mechanism primarily makes use of a range of chitinases, β-1,3-glucanases and proteases (Köhl et al., 2019). The *B*25 genome contains several genes that encode CWDEs: two chitinases (A and B), a chitosanase, and a glycoside hydrolase from the GH18 family (Douriet-Gámez et al., 2018). Biochemical characterisations of chitinases from *B*25 have revealed that both ChiA and ChiB function as exochitinases, although ChiB exhibits a dual substrate activity and also acts as an endochitinase (Morales-Ruiz et al., 2021). The gene expression patterns of chitinase genes (Figure 1D-E) determined here indicate that *BcChiB* is induced at 6 h, before *BcChiA* (at 12 h). This observation correlates well with the work of Figueroa-López et al. (2017), who showed that *ChiB* from *B*25 is induced earlier than *ChiA* when using colloidal chitin, or fungal lysate as a chitinase inducer.

In agreement with the induction of *BcChiB* found here, exochitinase and endochitinase activities were observed at 6 h in the *B*25 + *Fv* treatment. Although ChiA can display exochitinase activity, its activity is one hundred times lower than that of ChiB (Morales-Ruiz et al., 2021). Furthermore, no induction was found for the gene *BcChiA* at 6 h (Figure 1D), suggesting that ChiB is the key player in chitin degradation in the *B*25 + *Fv* interaction. These results also agree with the proposal that *B*25 ChiB is the main contributor to chitin degradation, since it displayed a higher enzymatic activity than ChiA (Morales-Ruiz et al., 2021). The high enzymatic activity of ChiB can be explained by the presence of two auxiliary functional domains: a carbohydrate binding domain (CBM 2), and a fibronectin type III domain (Fn3) that is only present in ChiB and not in ChiA (Figueroa-López et al., 2017). These domains could enhance the binding of the substrate and the stability of the enzyme (Morales-Ruiz et al., 2021). Taken together, the gene expression and the observed endochitinase and exochitinase activity patterns (Figure 1D-E; Table 3) support the idea that ChiA and ChiB could act synergistically, as proposed by Morales-Ruiz et al. (2021). In this example, ChiB would function as an endochitinase, randomly cleaving chitin chains at internal sites in the fungal cell wall, generating substrates for the subsequent exochitinase activity of both ChiB and ChiA (Morales-Ruiz et al., 2021).

Chitin, glucans, chitosan, mannans/galactomannans, and glycoproteins are the major components of the cell wall in some filamentous fungi (Aranda-Martinez et al., 2016). Chitosan is a highly de-acetylated form of chitin (Aranda-Martinez et al., 2016) that can be degraded by chitosanases. Furthermore, chitosanases from bacteria such as *Burkholderia gladioli* and *Streptomyces coelicolor* can act synergistically with chitinase to degrade the fungal cell wall (Gupta et al., 2012). Here, it was found that the induction of the chitosanase gene *BcCsn* overlaps in time with the induction of both chitinase genes (*BcCsn* remained induced from 6 h up to 30 h), as well as its enzymatic activity, which was observed in the CDA plates from 12 h to 30 h in the *B*25 + *Fv* treatment (Figure 1F; Table 4). On the other hand, *BcGH18* (endoglucanase) was only induced at 24 h, yet it overlaps with the induction of *BcCsn* at the same time (Figure 1G). Thus, it is possible that *B*25 lytic enzymes (chitinases, chitosanase and

endoglucanase) could act together in order to degrade the cell wall when confronted with the fungus.

Cell wall degradation was visualised by light and confocal laser microscopy observations made on samples from confrontation assay experiments (using *B*25 and a GFP-expressing *B*25 strain), where less hyphae branching and abnormal growth (thinning of the cell wall and swelling of the hyphae) could be seen (Figures 2 and 3; Table 2). Previously, our research group showed that *Fv* conidia that germinated in the presence of the purified *B*25 recombinant chitinases ChiA and ChiB were swollen, unbranched and smaller than the control (Morales-Ruiz et al., 2021). In addition, the purified chitinases A and B, alone or in combination, reduced the conidia germination of *Fv* (Morales-Ruiz et al., 2021). Here, we observed the same effect when conidia from *Fv* were germinated in the presence of the *B*25 and *B*25 + *Fv* supernatants obtained from the confrontation assay (mainly for supernatants from 24 and 30 h; Table 5).

In addition to the effect of lytic enzymes, biofilm formation and production of lipopeptide biosurfactants (LPs) such as surfactin, fengycin and iturin are traits linked to some BCAs (Chitarra et al., 2003; Pandin et al., 2017; Zhao et al., 2014). Some of the biocontrol mechanisms associated with biofilm includes: induced systemic resistance (ISR), antimicrobial-producing biofilm, plant growth promotion, niche exclusion, mechanical protection, competitive colonisation and mycelia colonisation (Pandin et al., 2017). For LPs three main natural functions have been described: antagonism towards other microorganisms, motility and attachment to surfaces (Raaijmakers et al., 2010). However, LPs also play a role in biofilm formation and development, plant pathogenesis and induction of ISR and chelation of metal ions and degradation of xenobiotics (Raaijmakers et al., 2010). Both surfactin production and biofilm formation have been associated with the biocontrol effect of *B. subtilis* over the plant pathogenic bacteria *Pseudomonas syringae* pv. tomato DC3000 (Bais et al., 2004). Our gene expression analysis showed that biofilm and surfactin genes were induced by *Fv* between 6 and 30 h (Figure 1H-L). The microscopy images suggest the adherence of *B*25 to *Fv* mycelia starting at 3 h (Figure 2), whereas the microtiter plate assay revealed biofilm formation from 24 h to 48 h, but only when *B*25 interacted with the fungus. Moreover, a significant induction was observed from 6 to 48 h compared to *B*25 alone (Figure 4). This indicates that the *B*25 biofilm formation response is elicited by the presence of *Fv*. In contrast to the results from the microtiter plate assay (Figure 4B), the microscopy results from the *B*25 control at 12 and 24 h suggest biofilm formation (Figure 2), although this could be due to differences in experimental condition. Among the various biofilm modes of action, which differ between BCAs, we suggest that the biofilm-associated biocontrol mechanism that seems to fit best in this work is mycelial colonisation (Pandin et al., 2017), according to the microscopy images (Figure 2). For *S. marcescens* UENF-22GI, it is suggested that massive biofilm formation could hinder the fungal growth of *Fusarium oxysporum* and *F. solani*, while also probably facilitating the colonisation and degradation of fungal cell walls (Matteoli et al., 2018). There is a similar scenario with the *B*25 + *Fv* interaction, since we observed the induction of CWDEs and biofilm genes, biofilm formation, and chitinase and chitosanase activity.

Previously, the presence of LPs such as fengycin, iturin and surfactin in the supernatant of different *Bacillus* species was shown to affect the germination of different fungi by increasing the permeability in the lipid membrane of spores, causing the loss

of essential macromolecules in addition to inducing mycelial damage (Chitarra et al., 2003; Liu et al., 2014; Zhao et al., 2014). Furthermore, surfactin from *Brevibacillus brevis* KN8 was shown to cause damage and inhibition of *Fv* hyphae *in vitro* via DNA and protein damage and the reduction of GSH content (Krishnan et al., 2019). In addition, surfactin can stimulate biofilm formation in *B. subtilis* (López et al., 2009). Thus, it is possible that besides its direct effect over *Fv*, surfactin could induce biofilm formation in *B*25. This is supported by gene expression and biofilm formation results. Taken all these results together, it is possible to suggest that the damage and inhibition to *Fv* hyphae and conidia observed here is not just an effect from the biofilm formation, CWDEs activity and/or siderophore production, but it may also include surfactin activity. However, chemical analysis, by HPLC or other methods, is still needed to demonstrate the production of surfactin in the *B*25 supernatant, which may be involved in the induction of biofilm formation and destabilisation of *Fv*.

Additionally, since both biofilm (Pandin et al., 2017) and LPs (Raaijmakers et al., 2010) are associated with ISR in plants, this mechanism is currently being addressed by our group using a tripartite system that includes the interaction of maize with *B*25 and *Fv*.

Taken together, our gene expression data, biochemical results, and microscopy observations suggest that *B*25 could use multiple mechanisms to inhibit the growth and development of *Fv* when these microorganisms interact together in an *in vitro* environment.

Acknowledgements

We thank Dr. Brandon Loveall of Improvence for English proofreading of the manuscript.

Disclosure statement

No potential conflict of interest was reported by the author(s).

Funding

This work was supported by CONACyT FOINS Fronteras de la Ciencia [grant number 2016-01-2510]. PABA was granted a PhD fellowship [grant number. 70883] from CONACyT, and JECA received Master's and PhD fellowships [grant number 934735] from CONACyT. PABA and JECA were both granted complementary fellowship support from IPN (BEIFI fellowship programme).

ORCID

Paúl Alán Báez-Astorga http://orcid.org/0000-0001-6193-8228
Jesús Eduardo Cázares-Álvarez http://orcid.org/0000-0002-6516-0625
Abraham Cruz-Mendívil http://orcid.org/0000-0001-7999-181X
Francisco Roberto Quiroz-Figueroa http://orcid.org/0000-0002-1950-4810
Ignacio Eduardo Maldonado-Mendoza http://orcid.org/0000-0001-9952-1508

References

Aranda, P. S., Lajoie, D. M., & Jorcyk, C. L. (2012). Bleach gel: A simple agarose gel for analyzing RNA quality. *Electrophoresis*, *33*(2), 366–369. https://doi.org/10.1002/elps.201100335

Aranda-Martinez, A., Lopez-Moya, F., & Lopez-Llorca, L. V. (2016). Cell wall composition plays a key role on sensitivity of filamentous fungi to chitosan. *Journal of Basic Microbiology*, *56*(10), 1059–1070. https://doi.org/10.1002/jobm.201500775

Auger, S., Krin, E., Aymerich, S., & Gohar, M. (2006). Autoinducer 2 affects biofilm formation by *Bacillus cereus*. *Applied and Environmental Microbiology*, *72*(1), 937–941. https://doi.org/10.1128/AEM.72.1.937-941.2006

Bacon, C. W., Yates, I. E., Hinton, D. M., & Meredith, F. (2001). Biological control of *Fusarium moniliforme* in maize. *Environmental Health Perspectives*, *109*(SUPPL. 2), 325–332. https://doi.org/10.2307/3435026

Bais, H. P., Fall, R., & Vivanco, J. M. (2004). Biocontrol of *Bacillus subtilis* against infection of *Arabidopsis* roots by *Pseudomonas syringae* is facilitated by biofilm formation and surfactin production. *Plant Physiology*, *134*(January), 307–319. https://doi.org/10.1104/pp.103.028712

Cavaglieri, L., Orlando, J., Rodríguez, M. I., Chulze, S., & Etcheverry, M. (2005). Biocontrol of *Bacillus subtilis* against *Fusarium verticillioides* in vitro and at the maize root level. *Research in Microbiology*, *156*(5–6), 748–754. https://doi.org/10.1016/j.resmic.2005.03.001

Cervantes-Gámez, R. G., Bueno-Ibarra, M. A., Cruz-Mendívil, A., Calderón-Vázquez, C. L., Ramírez-Douriet, C. M., Maldonado-Mendoza, I. E., Villalobos-López, MÁ, Valdez-Ortíz, Á, & López-Meyer, M. (2015). Arbuscular mycorrhizal symbiosis-induced expression ehanges in *Solanum lycopersicum* leaves revealed by RNA-seq analysis. *Plant Molecular Biology Reporter*, *34*(1), 89–102. https://doi.org/10.1007/s11105-015-0903-9

Cheng, C. Y., & Li, Y.-K. (2000). An *Aspergillus* chitosanase with potential for large-scale preparation of chitosan oligosaccharides. *Biotechnology and Applied Biochemistry*, *32*(3), 197. https://doi.org/10.1042/ba20000063

Chitarra, G. S., Breeuwer, P., Nout, M. J. R., Van Aelst, A. C., Rombouts, F. M., & Abee, T. (2003). An antifungal compound produced by *Bacillus subtilis* YM 10-20 inhibits germination of *Penicillium roqueforti* conidiospores. *Journal of Applied Microbiology*, *94*(2), 159–166. https://doi.org/10.1046/j.1365-2672.2003.01819.x

Covarelli, L., Stifano, S., Beccari, G., Raggi, L., Lattanzio, V. M. T., & Albertini, E. (2012). Characterization of *Fusarium verticillioides* strains isolated from maize in Italy: fumonisin production, pathogenicity and genetic variability. *Food Microbiology*, *31*(1), 17–24. https://doi.org/10.1016/j.fm.2012.02.002

Deepa, N., Nagaraja, H., & Sreenivasa, M. Y. (2016). Prevalence of fumonisin producing *Fusarium verticillioides* associated with cereals grown in karnataka (India). *Food Science and Human Wellness*, *5*(3), 156–162. https://doi.org/10.1016/j.fshw.2016.07.001

Douriet-Gámez, N. R., Maldonado-Mendoza, I. E., Ibarra-Laclette, E., Blom, J., & Calderón-Vázquez, C. L. (2018). Genomic analysis of *Bacillus* sp. strain B25, a biocontrol agent of maize pathogen *Fusarium verticillioides*. *Current Microbiology*, *75*(3), 247–255. https://doi.org/10.1007/s00284-017-1372-1

Dunlap, C. A., Schisler, D. A., Bowman, M. J., & Rooney, A. P. (2015). Genomic analysis of *Bacillus subtilis* OH 131 . 1 and co-culturing with *Cryptococcus flavescens* for control of Fusarium head blight. *Plant Gene*, *2*, 1–9. https://doi.org/10.1016/j.plgene.2015.03.002

Figueroa-López, A. M., Cordero-Ramírez, J. D., Martínez-Álvarez, J. C., López-Meyer, M., Lizárraga-Sánchez, G. J., Félix-Gastélum, R., Castro-Martínez, C., & Maldonado-Mendoza, I. E. (2016). Rhizospheric bacteria of maize with potential for biocontrol of *Fusarium verticillioides*. *SpringerPlus*, *5*(1), https://doi.org/10.1186/s40064-016-1780-x

Figueroa-López, A. M., Cordero-Ramírez, J. D., Quiroz-Figueroa, F. R., & Maldonado-Mendoza, I. E. (2014). A high-throughput screening assay to identify bacterial antagonists against *Fusarium verticillioides*. *Journal of Basic Microbiology*, *54*(SUPPL.1), 125–133. https://doi.org/10.1002/jobm.201200594

Figueroa-López, A. M., Leyva-Madrigal, K. Y., Cervantes-Gámez, R. G., Beltran-Arredondo, L. I., Douriet-Gámez, N. R., Castro-Martínez, C., & Maldonado-Mendoza, I. E. (2017). Induction of *Bacillus cereus* chitinases as a response to lysates of *Fusarium verticillioides*. *Romanian Biotechnological Letters*, *22*(4), 12722–12731.

Gupta, V., Prasanna, R., Srivastava, A. K., & Sharma, J. (2012). Purification and characterization of a novel antifungal endo-type chitosanase from *Anabaena fertilissima*. *Annals of Microbiology*, *62* (3), 1089–1098. https://doi.org/10.1007/s13213-011-0350-2

Jiang, C. H., Huang, Z. Y., Xie, P., Gu, C., Li, K., Wang, D. C., Yu, Y. Y., Fan, Z. H., Wang, C. J., Wang, Y. P., Guo, Y. H., & Guo, J. H. (2016). Transcription factors WRKY70 and WRKY11 served as regulators in rhizobacterium *Bacillus cereus* AR156-induced systemic resistance to *Pseudomonas syringae* pv. tomato DC3000 in *Arabidopsis*. *Journal of Experimental Botany*, *67* (1), 157–174. https://doi.org/10.1093/jxb/erv445

Köhl, J., Kolnaar, R., & Ravensberg, W. J. (2019). Mode of action of microbial biological control agents against plant diseases: relevance beyond efficacy. *Frontiers in Plant Science*, *10*(July), 1–19. https://doi.org/10.3389/fpls.2019.00845

Krishnan, N., Velramar, B., & Velu, R. K. (2019). Investigation of antifungal activity of surfactin against mycotoxigenic phytopathogenic fungus *Fusarium moniliforme* and its impact in seed germination and mycotoxicosis. *Pesticide Biochemistry and Physiology*, *155*(December 2018), 101–107. https://doi.org/10.1016/j.pestbp.2019.01.010

Lee, J. Y., Janes, B. K., Passalacqua, K. D., Pfleger, B. F., Bergman, N. H., Liu, H., Håkansson, K., Somu, R. V., Aldrich, C. C., Cendrowski, S., Hanna, P. C., & Sherman, D. H. (2007). Biosynthetic analysis of the petrobactin siderophore pathway from *Bacillus anthracis*. *Journal of Bacteriology*, *189*(5), 1698–1710. https://doi.org/10.1128/JB.01526-06

Lee, J. Y., Passalacqua, K. D., Hanna, P. C., & Sherman, D. H. (2011). Regulation of petrobactin and bacillibactin biosynthesis in *Bacillus anthracis* under iron and oxygen variation. *PLoS ONE*, *6*(6), https://doi.org/10.1371/journal.pone.0020777

Leyva-Madrigal, K. Y., Larralde-Corona, C. P., Apodaca-Sánchez, M. A., Quiroz-Figueroa, F. R., Mexia-Bolaños, P. A., Portillo-Valenzuela, S., Ordaz-Ochoa, J., & Maldonado-Mendoza, I. E. (2015). *Fusarium* species from the Fusarium fujikuroi species complex involved in mixed infections of maize in northern Sinaloa, Mexico. *Journal of Phytopathology*, *163*(6), 486–497. https://doi.org/10.1111/jph.12346

Leyva-Madrigal, K. Y., Sandoval-Castro, E., Calderón-Vázquez, C. L., Larralde-Corona, C. P., & Maldonado-Mendoza, I. E. (2017). Pathogenic and genetic variability of *Fusarium verticillioides* from maize in northern Mexico. *Canadian Journal of Plant Pathology*, *39*(4), 486–496. https://doi.org/10.1080/07060661.2017.1378726

Li, B., Li, Q., Xu, Z., Zhang, N., Shen, Q., & Zhang, R. (2014). Responses of beneficial *Bacillus amyloliquefaciens* SQR9 to different soilborne fungal pathogens through the alteration of antifungal compounds production. *Frontiers in Microbiology*, *5*(NOV), 1–10. https://doi.org/10.3389/fmicb.2014.00636

Liu, J., Hagberg, I., Novitsky, L., Hadj-Moussa, H., & Avis, T. J. (2014). Interaction of antimicrobial cyclic lipopeptides from *Bacillus subtilis* influences their effect on spore germination and membrane permeability in fungal plant pathogens. *Fungal Biology*, *118*(11), 855–861. https://doi.org/10.1016/j.funbio.2014.07.004

Livak, K. J., & Schmittgen, T. D. (2001). Analysis of relative gene expression data using real-time quantitative PCR and the 2-ΔΔCT method. *Methods*, *25*(4), 402–408. https://doi.org/10.1006/meth.2001.1262

Lizárraga-Sánchez, G. J., Leyva-Madrigal, K. Y., Sánchez-Peña, P., Quiroz-Figueroa, F. R., & Maldonado-Mendoza, I. E. (2015). *Bacillus cereus sensu lato* strain B25 controls maize stalk and ear rot in Sinaloa, Mexico. *Field Crops Research*, *176*, 11–21. https://doi.org/10.1016/j.fcr.2015.02.015

López, D., Fischbach, M. A., Chu, F., Losick, R., & Kolter, R. (2009). Structurally diverse natural products that cause potassium leakage trigger multicellularity in *Bacillus subtilis*. *Proceedings of the National Academy of Sciences of the United States of America*, *106*(1), 280–285. https://doi.org/10.1073/pnas.0810940106

Madania, A., Altawil, M., Naffaa, W., Volker, P. H., & Hawat, M. (2013). Morphological and molecular characterization of *Fusarium* isolated from maize in Syria. *Journal of Phytopathology*, *161* (7–8), 452–458. https://doi.org/10.1111/jph.12085

Martínez-Álvarez, J. C., Castro-Martínez, C., Sánchez-Peña, P., Gutiérrez-Dorado, R., & Maldonado-Mendoza, I. E. (2016). Development of a powder formulation based on *Bacillus cereus sensu lato* strain B25 spores for biological control of *Fusarium verticillioides* in maize plants. *World Journal of Microbiology and Biotechnology*, *32*(5), https://doi.org/10.1007/s11274-015-2000-5

Maschietto, V., Lanubile, A., De Leonardis, S., Marocco, A., & Paciolla, C. (2016). Constitutive expression of pathogenesis-related proteins and antioxydant enzyme activities triggers maize resistance towards *Fusarium verticillioides*. *Journal of Plant Physiology*, *200*, 53–61. https://doi.org/10.1016/j.jplph.2016.06.006

Matteoli, F. P., Passarelli-Araujo, H., Reis, R. J. A., Da Rocha, L. O., De Souza, E. M., Aravind, L., Olivares, F. L., & Venancio, T. M. (2018). Genome sequencing and assessment of plant growth-promoting properties of a *Serratia marcescens* strain isolated from vermicompost. *BMC Genomics*, *19*(1), 1–19. https://doi.org/10.1186/s12864-018-5130-y

Morales-Ruiz, E., López-Ceballos, A., & Maldonado-Mendoza, I. E. (2019). Transformation of the rhizospheric *Bacillus cereus sensu lato* B25 strain using a room-temperature electrocompetent cells preparation protocol. *Plasmid*, *105*(February), 102435. https://doi.org/10.1016/j.plasmid.2019.102435

Morales-Ruiz, E., Priego-Rivera, R., Figueroa-López, A. M., Cazares-Álvarez, J. E., & Maldonado-Mendoza, I. E. (2021). Biochemical characterization of two chitinases from *Bacillus cereus sensu lato* B25 with antifungal activity against Fusarium verticillioides P03. *FEMS Microbiology Letters*, *368*(2), 1–8. https://doi.org/10.1093/femsle/fnaa218

Naumann, T. A., Wicklow, D. T., & Price, N. P. J. (2011). Identification of a chitinase-modifying protein from *Fusarium verticillioides*: truncation of a host resistance protein by a fungalysin metalloprotease. *Journal of Biological Chemistry*, *286*(41), 35358–35366. https://doi.org/10.1074/jbc.M111.279646

Pandin, C., Le Coq, D., Canette, A., Aymerich, S., & Briandet, R. (2017). Should the biofilm mode of life be taken into consideration for microbial biocontrol agents? *Microbial Biotechnology*, *10*(4), 719–734. https://doi.org/10.1111/1751-7915.12693

Raaijmakers, J. M., de Bruijn, I., Nybroe, O., & Ongena, M. (2010). Natural functions of lipopeptides from *Bacillus* and *Pseudomonas*: more than surfactants and antibiotics. *FEMS Microbiology Reviews*, *34*(6), 1037–1062. https://doi.org/10.1111/j.1574-6976.2010.00221.x

Raymaekers, K., Ponet, L., Holtappels, D., Berckmans, B., & Cammue, B. P. A. (2020). Screening for novel biocontrol agents applicable in plant disease management – A review. *Biological Control*, *144*(September 2019), 104240. https://doi.org/10.1016/j.biocontrol.2020.104240

Reiter, L., Kolstø, A. B., & Piehler, A. P. (2011). Reference genes for quantitative, reverse-transcription PCR in *Bacillus cereus* group strains throughout the bacterial life cycle. *Journal of Microbiological Methods*, *86*(2), 210–217. https://doi.org/10.1016/j.mimet.2011.05.006

Reyes-ramírez, A., Escudero-Abarca, B. I., Aguilar-Uscanga, G., Hayward-Jones, P. M., & Barboza-Corona, J. E. (2006). Antifungal activity of *Bacillus thuringiensis* chitinase and its potential for the biocontrol of phytopathogenic fungi in soybean seeds. *Journal of Food Science*, *69*(5), M131–M134. https://doi.org/10.1111/j.1365-2621.2004.tb10721.x

Schiessl, K. T., Janssen, E. M. L., Kraemer, S. M., McNeill, K., & Ackermann, M. (2017). Magnitude and mechanism of siderophore-mediated competition at low iron solubility in the *Pseudomonas aeruginosa* pyochelin system. *Frontiers in Microbiology*, *8*(OCT), 1–11. https://doi.org/10.3389/fmicb.2017.01964

Shu, X., Livingston, D. P., Woloshuk, C. P., & Payne, G. A. (2017). Comparative histological and transcriptional analysis of maize kernels infected with *Aspergillus flavus* and *Fusarium verticillioides*. *Frontiers in Plant Science*, *8*(December), 1–14. https://doi.org/10.3389/fpls.2017.02075

Zhao, Y., Selvaraj, J. N., Xing, F., Zhou, L., Wang, Y., Song, H., Tan, X., Sun, L., Sangare, L., Folly, Y. M. E., & Liu, Y. (2014). Antagonistic action of *Bacillus subtilis* strain SG6 on *Fusarium graminearum*. *PLoS ONE*, *9*(3), 1–11. https://doi.org/10.1371/journal.pone.0092486